DEPENDENCE BETWEEN SHOCK AND SEPARATION BUBBLE IN A SHOCK WAVE/BOUNDARY LAYER INTERACTION

J.F. DEBIÈVE, P. DUPONT
Institut Universitaire des Systèmes Thermiques Industriels, Université de Provence and UMR CNRS N°6595, 5 rue Enrico Fermi 13 Marseille Cedex 13, debieve@polytech.univ-mrs.fr

Abstract. We present experimental results obtained in a turbulent boundary layer at a Mach number of 2.3 impinged by an oblique shock wave. Strong unsteadinesses are developed in the interaction, involving several frequency ranges which can extend over two orders of magnitude. In this paper, attention is focused on the links between the low frequencies shock motions and the separation bubble. An interpretation based on a simple scheme of the longitudinal evolution of the instantaneous pressure is proposed. As it is mainly based on the pressure signals properties inside the region of the shock oscillation, it may be expected that it will be still relevant for different configurations of shock induced separation as compression ramp, blunt bodies or over expanded nozzles.

Key words: shock wave, boundary layer separation, unsteadiness

1.Introduction

Shock wave boundary layer interactions occur in various aeronautical applications: for example, in inlets of supersonic aircrafts or in over expanded nozzles. Depending on the geometry of the problem, different kind of interactions can be found. An important family of shock wave interaction is the case where the boundary layer separates because of the adverse pressure gradient produced by the shock wave and reattaches downstream. In these cases, a limited region of the flow becomes subsonic downstream the shock wave, allowing spatial couplings through the pressure between different regions of the interaction. Such a behavior involves, for example, flows as compression ramps, incident shock waves, blunt fins or over expanded nozzles in restricted separation cases. In all these separated cases, new unsteadinesses are developed. They involve a large number of time scales, which can be at least one or two orders of magnitude larger than the energetic time scales of the upstream boundary layer. Several pioneering works, [1, 2], and more recent experimental studies [3, 4, 5] have shown that these flows exhibit very low frequency shock motions as well as the development of new large scales downstream the separation point. Recent works [6, 7] have shown that, independently of the particular spatial organization of these interactions (compression ramp, incident shock, blunt fin...) a typical dimensionless frequency, or Strouhal number, can be associated with these low frequency shock

movements. Nevertheless, the origin of these unsteadinesses are not yet well understood. Two scenarii can be considered:

- ✔ the shock motions can be driven by some upstream low frequency events
- ✔ or they can be driven by some low frequency downstream events from the subsonic separated region.

Both scenarii can be expected, with possibly some couplings between them. In that respect, evidences of upstream or downstream dependances have been obtained in compression ramps [2, 8, 9, 10] and in shock wave reflection [7, 11]. Some of these experimental results have shown statistical links between signals associated to the shock motions and the separated bubble. The aim of this paper is to examine the spatial and temporal dependences between the shock movements and the separated bubble. From the different experimental observations, we developed a simple scheme able to reproduce the spatial and temporal wall pressure evolutions inside the interaction. To develop this scheme, we will consider unsteady wall pressure measurements together with instantaneous velocity fields obtained recently by PIV measurements in the case of an incident shock wave. The output of the scheme will be compared with experimental observations such as longitudinal evolution of mean wall pressure, standard deviation and phase shift between pressure signals recorded in different region of the interaction. As it is mainly based on the description of wall pressure variation in the vicinity of the foot of the unsteady detached shock, some generality can be expected for different cases such as compression ramp or blunt fins.

2.Experimental set up and description of the flow unsteadiness

The experiment was carried out in the hypo-turbulent supersonic wind tunnel at IUSTI. It is a continuous facility with a closed-loop circuit. The nominal conditions of the interaction are summarized in table 1.

M	U_0	δ_0	R_e	C_f	T_t
2,3	$550 m.s^{-1}$	11mm	6.9×10^3	2×10^{-3}	300K

Table 1. Aerodynamic parameters of the flow upstream of the interaction.

A shock generator is fixed on the ceiling of the wind tunnel. The flow deviation can be set to 8 and 9,5°. The length of interaction L is defined as the distance between the foot of the reflected shock (X_0) and the extrapolation down to the wall of the incident shock. The dimensionless coordinate is therefore $X^*=(x-X_0)/L$, and the interaction extends from $X^*=0$ to 1. The global organisation of the incident shock wave boundary layer interaction obtained by spark Schlieren visualisation is presented in Fig.1. The flow deviation due to the incident shock is 8°, and the pressure gradient is strong enough for the layer to separate. In this case, the reflected shock which originates upstream of the recirculating zone is

known to be strongly unsteady with low frequencies oscillations of several hundreds of Hertz [4, 12]. A dimensionless frequency, or Strouhal number, defined by $S_L=fL/U_\infty$, where U_∞ is the external velocity, has been used to compare the different shock induced separated flows [6, 7]. In all cases, very low Strouhal numbers are obtained: S_L is of the order of 0,03. PIV measurements[11] highlighted the development, inside the recirculating zone, of high energetic structures. These structures have been shown to be generated in the mixing layer which develops from the separation point. They correspond to frequencies one order of magnitude lower than the energetic eddies in the upstream boundary layer, as in subsonic separations. Superimposed on these ones, frequencies of one order of magnitude below (in the same range as the characteristic frequencies associated with the reflected shock motions) have been identified in the interaction zone. These low frequencies correspond to a Srouhal number S_L ~0.03, therefore they cannot be compared directly with low frequencies observed in subsonic detached flows, generally associated to some "flapping" phenomena of the mixing layer, involving Strouhal number of about 0.12[13].

Hereafter only the low passed signal associated with this range of frequencies is taken into account. These low frequencies are found in almost linear dependence with the reflected shock signal: the coherence function between the pressure in the vicinity of the unsteady reflected shock and pressure in the separation where $0.5<X^*<1$ keep a significant value close to one (see figure 2). For sake of comparison, we have also shown in this figure the low level of coherence between the shock and the initial boundary layer for the case $\theta=8°$. Moreover, the wall pressure signals of the reflected shock and the downstream flow are found in phase opposition: the pressure in the bubble drops down when the shock is in an upstream position and conversely. This phase opposition is illustrated on figure n°3, where the intercorrelation functions between the low pass signals taken simultaneously at the mean position of the reflected shock ($X^*=0$), and inside the recirculating zone ($0.5<X^*<1$), are plotted in the case $\theta=8°$. A strong negative value at the optimal delay time can be observed. We have also reported results with the downstream relaxation ($X^*>1$), where the intercorrelation vanishes progressively.

Moreover, one can remark that the optimal delay time of the intercorrelation function is nearly equal to zero for $X^*<1$, which means that the instantaneous pressure variations due to the shock motions are simultaneous with the pressure variations in the recirculating bubble. More precisely, the ratio of this delay time to the characteristic time scale for the phenomenon variation which is the time scale of the shock excursion (i.e. The inverse of the shock dominant frequency), is presented on figure n°4. This ratio is negligible in the recirculating bubble ($X^*<1$). For the strongest shock $\theta=9.5°$, some similar results are obtained. Signals are found in phase opposition with zero delay time near the reattachment point ($X^*=1$), see figure n°4. So, as in the 8° case, the link between the reattachment region and the reflected shock movements is quasi instantaneous, even compared to an acoustic time defined as L/a or a convection time L/U_∞. This means that the instantaneous pressure variations due to the shock movements are simultaneous with the pressure variations at these points and are not related through any propagative or convective scheme along the longitudinal direction.

On the other hand, for the case θ=9.5°, snon-zero, negative optimal delay times can be observed in the recirculating bubble (see figure 4). Therefore, it seems that, in this case, some propagative or convective scales are over imposed to the global pulsation of the recirculating bubble. In both cases, this strong link becomes weaker downstream in the relaxation zone.

3.Links between shock motions and the separated region

Previous works have already put in evidence strong statistical links between the low frequency shock movements and the flow which develops downstream in various shock induced configurations. Most of these results have been derived from unsteady wall measurements. For example, in a compression ramp at M=1.5, Thomas [2] finds a strong coherence between the wall pressure fluctuations recorded near the mean position of the foot of the separation shock and recorded near the reattachment point. Moreover, he observed that signals where in phase opposition. Similar results were obtained in a M=5 compression ramp [10]. Nevertheless, these finding were only deduced from wall pressure measurements, so that the aerodynamic interpretation are rather difficult.
More recently, [9, 11] PIV measurements in compression ramp and incident shock wave have confirmed these results. In the case of the incident shock wave, evidences of dependence between the shock movements, with large amplitude vertical displacement of the recirculating bubble have been given. A model based on such behavior has been proposed by Thomas et al. to explain the phase opposition in the case of ramp compression. The main point of the model is the observation of a specific pattern on the instantaneous pressure repartitions at the reattachment points producing some unsteady signals when the recirculating bubble is contracting or dilating. Nevertheless in our case of incident shock wave, no particular trend on the pressure fluctuation is observed near the reattachment point, and the scheme cannot be directly used. Moreover, it is difficult with Thomas' interpretation to explain the phase opposition between the shock signal and any point inside the recirculating bubble. In the next part, we modify this starting point, and we propose a simple model describing the longitudinal instantaneous wall pressure repartitions.

1.2. INSTANTANEOUS WALL PRESSURE SCHEME

Our objective is to define the simplest model for the longitudinal instantaneous wall pressure repartition and its variations when the reflected shock moves, compatible with the experimental observations. As the delay time of influence is negligible in respect of the time scale of the phenomenon, and as signals are nearly linearly related (Coherence≈1) the instantaneous longitudinal pressure repartitions can be expressed in a one-to-one correspondence with the instantaneous movements of the reflected shock around its mean

position, i.e. a function of the position of the focused shock.
The time history of the wall pressure near the foot of the unsteady reflected shock is reported figure in 5 for two different positions inside the region of shock oscillations. The upstream shock displacements correspond to the positive rises and the downstream ones are associated with the negative steps. In this figure, the upstream wall pressure and the pressure step given by the inviscid theory is also given for the considered case (θ=9.5°). It is clear that, at least near the wall, a model based on a single focused shock wave cannot be sufficient to describe the pressure signals. Only about the half of the pressure increase can be associated with a shock-like increase, when the rest corresponds to a progressive longitudinal increase of pressure. From these observations, we define our model with the following characteristics:

- ➔ firstly, the step of pressure through the focused shock is constant but less than the theoretical total increase of pressure
- ➔ secondly, the levels of pressure at the point of the focused shock depends on its position.

Then, a crude scheme describing these signals can be as follows:

- ✔ a constant pressure p_0 upstream the region of shock oscillations
- ✔ a longitudinal pressure gradient in the region of oscillation, defined from the offset of the signals plotted figure 5
- ✔ a constant step of pressure starting from the current pressure upstream of the shock position. This upstream pressure depends on the instantaneous position of the shock wave. This step of pressure is about the half of the total increase pressure downstream of the shock wave with respect to the infinite upstream pressure p_0.
- ✔ downstream the instantaneous shock wave, the recirculating zone is developing: it is mimicked by a constant adverse pressure gradient deduced, for example, from the mean pressure measurements.

This leads to the global scheme which is detailed on the figure 6, with four main parameters:

- ✔ L_{ex} : length of the region of shock oscillations
- ✔ Δp : step of pressure through the focused wave
- ✔ $\partial p_1/\partial x$: longitudinal pressure gradient in the region of shock oscillations
- ✔ $\partial p_2/\partial x$: longitudinal pressure gradient in the recirculating zone
- ✔ finally, the probability density function of the shock presence on the excursion length L_{ex} is supposed to be Gaussian.

The different parameters are deduced from experimental signals. The length of oscillations L_{ex} is derived from the longitudinal evolution of the standard deviation of the wall pressure fluctuations [12]: $L_{ex}/L \approx 0{,}3$.
The residual adverse pressure gradient is defined as a linear increase of the pressure immediately upstream of the shock wave, starting at the beginning of the oscillation zone of the shock. The step of pressure Δp and the residual pressure gradient $\partial p_1/\partial x$ are deduced from the experimental signals ($\Delta p/Dp$=0,53 , where Dp is the the incident shock pressure

step) and the pressure gradient such as the mean pressure reaches the right level at the end of the intermittent shock region. Finally, the pressure gradient inside the recirculating zone, $\partial p_2/\partial x$, is deduced from the mean wall pressure slope in this region. With these four parameters, the model is fully defined. In the next section, comparisons with experimental results are presented.

1.3. COMPARISON WITH EXPERIMENTAL RESULTS

From this scheme we can obtain statistical informations on the pressure repartitions, which depend only on the position of the moving shock. A random simulation with a Gaussian law leads to the mean, rms, phase of the pressure. We show in figure 7 that the simulated mean pressure reproduces conveniently the experiments. The instantaneous repartitions are smoothed by the weighting action of the shock intermittency. In figure 7, we check, for the case at θ=9.5°, that the simulated rms pressure level reproduces in a satisfactory way the rms value σ_p of low passed pressure signals. We will detail now some results which can be found in some particular points and the comparison with the equivalent experimental results.

1. *The maximum level of pressure fluctuations*

The maximum of the rms pressure is located near of the median position of the shock (X*=0), where the intermittency coefficient γ =1/2 and its value is in our case $p'^*=\sigma_p/\Delta p\sim 0.43$, which can be compared to the experimental value (0,34). With this model, it may be retained that the maximum of pressure fluctuations, in the intermittency zone, is proportional to the step of pressure for the focused part of the reflected shock.

2. *Level of rms pressure downstream the shock oscillations*

Downstream of the intermittent zone the model leads to a fluctuation level such as:

$$\sigma_p = |\partial p_1/\partial x - \partial p_2/\partial x|\,\sigma_c$$

where σ_c is the rms values for the shock position excursions. From this expression or from the simulations (figure 7), typical values compared to the incident shock pressure step are σ_p/Dp=10% (case θ=9.5°). This model indicates also that the pressure fluctuation level for the low frequency range, in the recirculating bubble, is proportional to the slope difference ($\partial p_1/\partial x - \partial p_2/\partial x$) of the unfocused compressions and is also proportional to the length scale of the reflected shock motion.

3. *Phase shift between the reflected shock and the recirculating bubble*

The phase shift between the pressure signals at the foot of the shock and in the recirculating bubble can be deduced from the model. The fluctuations correspond to the difference between the instantaneous pressure (thick line in figure 8) and the mean pressure (thin line). In the simplified case of a periodic shock motion, a reconstruction of the temporal signal (in arbitrary scales) for two points placed respectively at the mean position of the reflected shock and in the recirculating bubble, is presented figure 8. They are in phase opposition, which is in agreement with the experimental results.

We can notice that the two cases of in-phase or out-of- phase signals are defined by the sign of the slope difference ($\partial p_1/\partial x - \partial p_2/\partial x$). Therefore, a shock model as an Heaviside

distribution with constant plateau downstream the shock $\partial p_1/\partial x - \partial p_2/\partial x = 0$ does not leads to a phase opposition between the two signals.
The proposed scheme for the low passed wall pressure behavior in the interaction synthesizes the different experimental observations. However, it is only descriptive, it does not explain the shock decomposition in two part in the intermittent zone: about one half for a focused shock, and another half with an continuous compression. This hypothesis is the basic point for the explanation of the phase opposition phenomena or for the low passed residual pressure fluctuation level in the recirculating bubble.

4.Conclusions

The present results give a preliminary overview on unsteadiness for an incident shock wave induced separation, with different shock intensities. We propose for the wall pressure repartition, in a low frequency range, a very simplified scheme for the wall pressure repartition able to synthesize the various experimental observations. Experiments show that the link between the low frequency shock motions and the vicinity of the reattachment is quasi instantaneous, quicker than an acoustic propagation or convection in a streamwise direction. This leaves the possibility of a global perturbed motion in the other directions. So, the analysis of the stability of such a system would be of great interest. The possibility of an excitation of the system by perturbations coming from the upstream turbulent boundary layer could also be considered.

Acknowledgements

Part of this work was carried out with the support of the Research Pole ONERA/CNES *Aérodynamique des Tuyères et Arrière-Corps* (ATAC) and of the European STREP UFAST. Their support is gratefully acknowledged. Comments of Dr. J.P. Dussauge are also gratefully acknowledged.

References

1. Dolling D.S., Fifty years of shock-wave/boundary-layer interaction research: what next, AIAA Journal, Vol. 39, n°8, pp.1517-1531, 2001.
2. Thomas F.O., Putman C.M., CHU H.C., On the mechanism of unsteady shock oscillation in shock wave/turbulent boundary layer interaction, Experiments in Fluids, Vol. 18, pp.69-81, 1994.
3. Nguyen A.T., Deniau H., Girard S., Alziary de Roquefort T., Wall pressure fluctuations in an over-expanded supersonic nozzle, 38th AIAA Joint Propulsion Conference, Indianapolis, AIAA Paper, 02-4001, , 2002.

4. Haddad C., Instationnarités, mouvements d'onde de choc et tourbillons à grande échelles dans une interaction onde de choc/couche limite avec décollement, Université de Provence Aix-Marseille I, Thèse de Doctorat, 2005.
5. Dupont P., Haddad C., Ardissone J.P., Debiève J.F., Instationnarités et structures à grande échelle dans une interaction onde de choc - couche limite avec décollement, Recherche aéronautique sur le supersonique, premier appel à proposition, Rapport Final, 2003.
6. Dussauge J.P., Dupont P., Debiève J.F., Unsteadiness in shock wave boundary layer interactions with separation, Aerospace Science and Technology, Vol. 10, pp.85-91, 2006.
7. Dupont P., Haddad C., Debiève J.F., Space and time organization in a shock induced boundary layer, J. Fluid Mech., Vol. 559, pp.255-277, 2006.
8. Ünalmis Ö.H., Dolling D.S., Experimental study of causes of unsteadiness of shock-induced turbulent separation, AIAA Journal, Vol. 36, N°3, pp.371-378, 1998.
9. Ganapathisubramani B., Clemens N., Dolling D., Effects of upstream coherent structures on low-frquency motion of shock-induced turbulent separation, 45th AIAA Aerospace Sciences Meeting and Exhibit, Reno, Nevada, 8-11 January, , 2007.
10. Erengil M.E., Dolling D.S., Unsteady wave structure near separation in a Mach 5 compression ramp interaction, AIAA Journal, Vol. 29, N°5, pp.728-735, 1991.
11. P. Dupont, S. Piponniau, A. Sidorenko and J.F. Debiève, Investigation of an Oblique Shock Reflection with Separation by PIV Measurements, 45th AIAA Aerospace Sciences Meeting and Exhibit, , 2007.
12. Dupont P., Haddad C., Ardissone J.P., Debiève J.F., Space and time organisation of a shock wave/turbulent boundary layer interaction, Aerospace Science and Technology, Vol. 9, Issue 7, pp.561-572, 2005.
13. Kiya M., Sasaki K., Structure of a turbulent separation bubble, J. Fluid Mech., Vol. 137, pp.83-113, 1983.

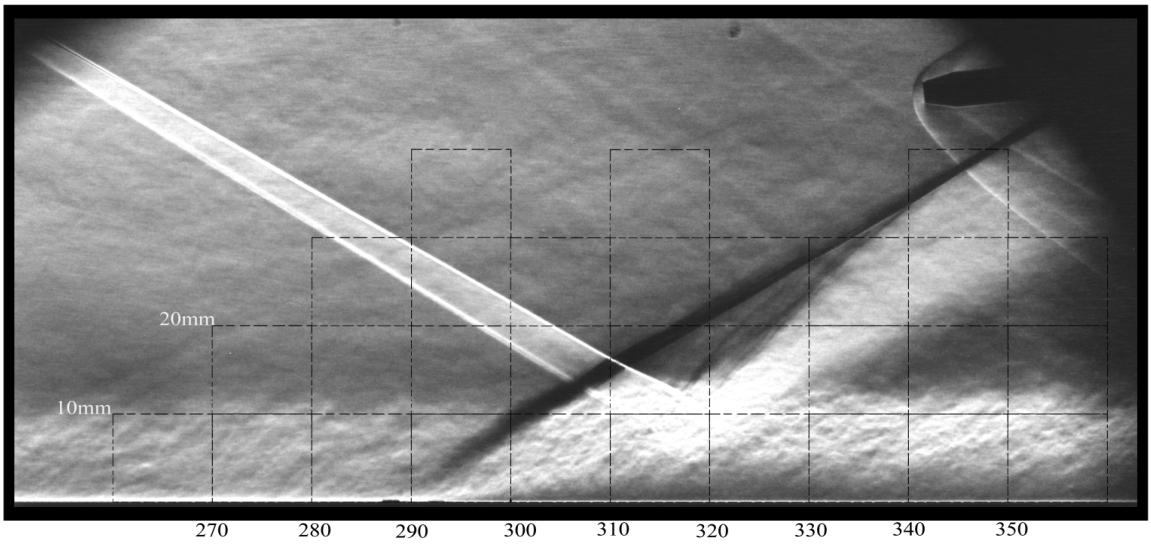

Figure 1. Spark Schlieren visualization of the interaction, flow deviation of 8°.

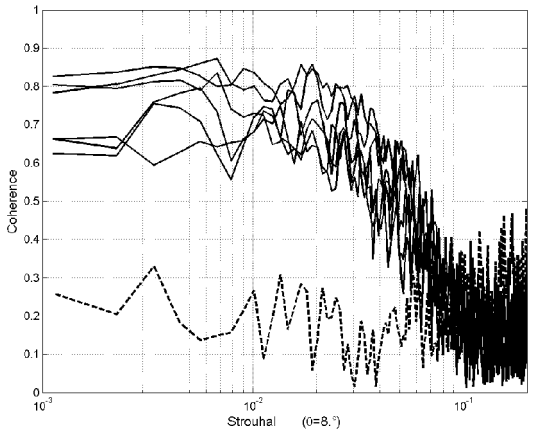

Figure 2: Coherence between pressure fluctuations near the reflected shock and the downstream flow (solid lines) and the upstream boundary layer (dashed line), in the case θ=8°.

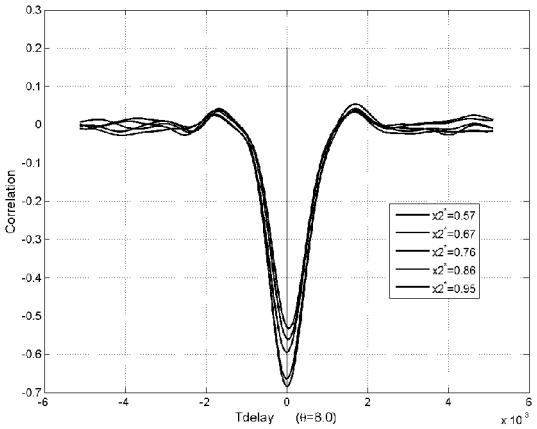

Figure 3: Intercorrelation function between wall pressure signals near the reflected shock and in the recirculating zone (X<1), θ=8°.*

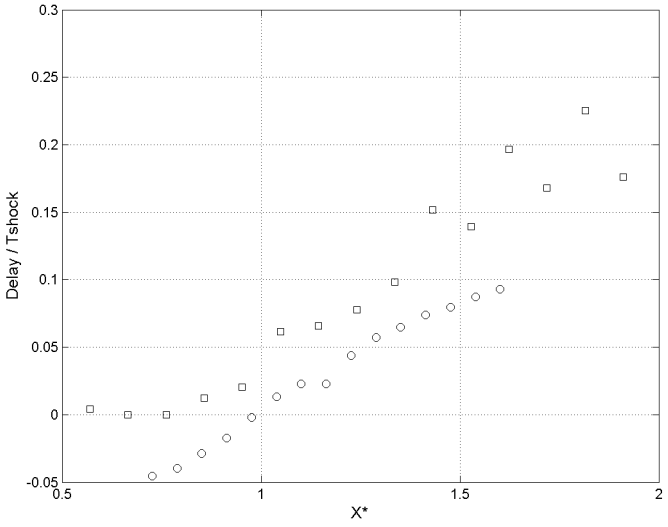

Figure 4: Ratio of the optimal delay time deduced from the intercorrelation functions to the characteristic time of the reflected shock movements, (□)θ=8°, (○)θ=9,5°.

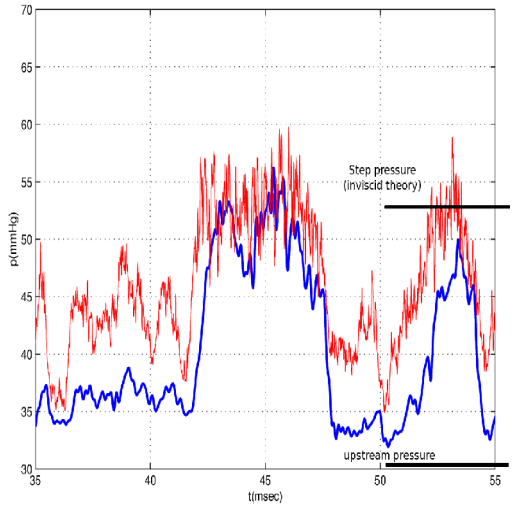

Figure 5: Wall pressure signals for different position near the mean position of the foot of the reflected shock.

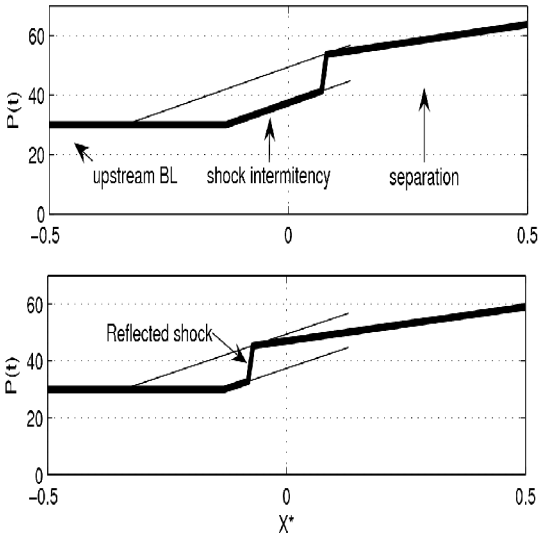

Figure 6: Unsteady shock scheme: shock motions in upstream and downstream directions.

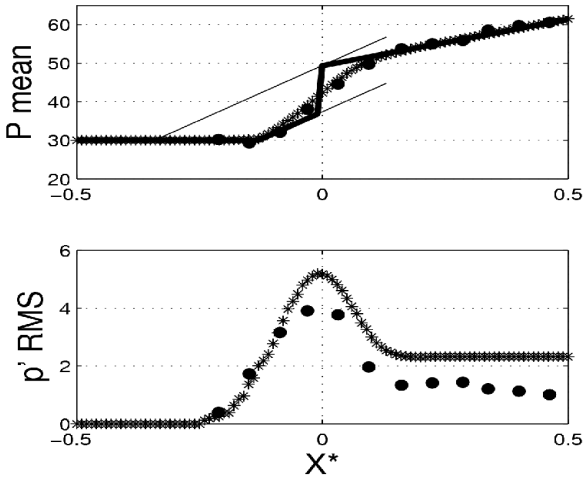

Figure 7: Comparison between the output of the pressure scheme and the experimental mean and standard deviation of the wall pressure;
*— instantaneous pressure (scheme); • experiments (pass-band on low frequencies shock motion); * scheme results.*

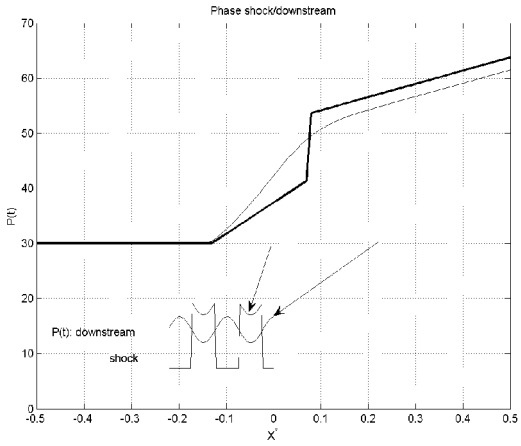

Figure 8: : instantaneous phase opposition between signals recorded at the foot of the shock (X=0) and in the recirculating bubble (X*=0,22).*